Research Article/Chemical, Environmental, and Food Engineering http://doi.org/10.15446/ing.investig.113022

Assessing the Interaction between Water Erosion and SOC Storage in a Small Mexican Watershed

Evaluación de la interacción entre la erosión hídrica y el almacenamiento de COS en una microcuenca mexicana

Olimpya T. Aguirre-Salado [1], Joel Pérez-Nieto [2], Carlos A. Aguirre-Salado [3], and Alejandro I. Monterroso-Rivas [4]

ABSTRACT

Water erosion is a significant issue that impacts a substantial portion of Mexico. The purpose of this study is to establish a connection between soil erosion and soil organic carbon (SOC) reserves. This work was conducted within a small watershed in the Mixteca Alta region of Oaxaca, in order to examine the correlation between erosion intensity, determined via the revised universal soil loss equation (RUSLE), and SOC storage, calculated using spatial models. The results reveal erosion values between 0.19 and 266.99 Mg ha^{-1} year^{-1}, with 305 693 t of erosion in the micro-watershed. The erosion patterns are closely linked to land use categories. The average SOC values (in Mg ha^{-1}) were associated with erosion, which was reclassified as null (31.79), light (22.36), moderate (16.19), and high (5.22). Kendall's *tau* coefficient showed a negative correlation of -0.39 between erosion and SOC. This inverse relationship can be attributed to the influence of erosive processes on the transport and exposure of SOC, the later replacement of carbon in the vegetation, and a reduced decomposition in deposition areas. Therefore, conservation practices, particularly terracing, have the potential to improve carbon storage.

Keywords: RUSLE, Kendall's tau coefficient, conservation practices, terracing, soil carbon stock

RESUMEN

La erosión hídrica es un problema significativo que afecta gran parte de México. El propósito de este estudio es establecer una conexión entre la erosión del suelo y las reservas de carbono orgánico del suelo (COS). Este trabajo fue realizado dentro de una pequeña cuenca hidrográfica en la región Mixteca Alta de Oaxaca para evaluar la correlación entre la intensidad de la erosión, determinada a través de la ecuación universal de pérdida de suelo revisada (RUSLE), y el almacenamiento del COS, calculado mediante modelado espacial. Los resultados revelan valores de erosión entre 0.19 y 266. 99 Mg ha^{-1} año^{-1}, con una erosión total de 305 693 t en la microcuenca. Los patrones de erosión están estrechamente vinculados a las categorías de uso del suelo. Los valores promedio de COS (en Mg ha^{-1}) se asociaron a la erosión, reclasificada como nula (31.79), ligera (22.36), moderada (16.19) y alta (5.22). El coeficiente *tau* de Kendall mostró una correlación negativa de -0.39 entre la erosión y el COS. Esta relación inversa puede atribuirse a la influencia de los procesos de erosión en el transporte y la exposición del COS, el posterior reemplazo de carbono de la vegetación y la reducción de la descomposición en las áreas de depósito. Por lo tanto, las prácticas de conservación, en particular las terrazas, tienen potencial para mejorar el almacenamiento de carbono.

Palabras clave: RUSLE, coeficiente tau de Kendall, prácticas de conservación, terrazas, almacenamiento de carbono en suelo

Received: February 18th, 2025
Accepted: May 19th, 2025

Introduction

Soil erosion entails soil displacement due to factors such as rain, runoff, wind, and gravity, leading to its deposition in depressions or water bodies [1]. This escalating issue threatens soil quality and environmental functions. Erosion contributes to organic matter (OM) loss through quicker decomposition and export from eroded sites [2]. Water erosion follows a four-stage process: initiation, splashing, transportation, and redistribution – as well as eventual deposition in depressions or water bodies [3]. This form of erosion is extremely damaging and leads to significant

[1] MSc in Hydrosciences, Colegio de Postgraduados, Mexico. Affiliation: Doctoral student, Universidad Autónoma Chapingo, Mexico. Email: oaguirres@chapingo.mx
[2] PhD in Soil Science, Colegio de Postgraduados, México. Affiliation: Professor (full), Universidad Autónoma Chapingo, Mexico. Email: jperezn@chapingo.mx
[3] PhD in Natural Resource Management, Universidad Autónoma de Nuevo León, México. Affiliation: Professor (full), Universidad Autónoma de San Luis Potosi, Mexico. ORCID: Email: carlos.aguirre@uaslp.mx
[4] PhD in Geography, Universidad Nacional Autónoma de México, México. Affiliation: Professor (full), Universidad Autónoma Chapingo, México. Email: aimrivas@correo.chapingo.mx

land degradation and nutrients, soil organisms, and organic carbon transport, thereby altering ecosystems.

Soil organic carbon (SOC) is the carbon that remains in the soil after the partial decomposition of organic matter [4]. Global SOC estimates range from 1500 to 2400 Pg C, making the soil the second-largest carbon reservoir [1]. SOC's relevance lies in its role in climate change mitigation through photosynthesis, which captures atmospheric carbon in the soil for long-term storage [5]. However, whether soil acts as a carbon sink or source depends on the SOC formation and decomposition rates.

[6] highlighted that approximately 50% of the SOC is concentrated within the upper 20-30 cm of soil depth. This implies that the first meter of soil holds two to three times more carbon than the atmosphere and Earth's entire vegetation combined [5]. Considering that water erosion displaces the topsoil, which is where most of the SOC is typically found, it is evident that this phenomenon has the potential to significantly impact SOC stocks. [7] explained that erosion processes modify SOC inventories by transporting SOC-enriched sediment away from a given landscape unit. Consequently, these processes not only result in the oxidation of SOC stocks and the release of carbon dioxide (CO_2) into the atmosphere; they also lead to SOC loss via surface runoff. Hence, erosion essentially redistributes SOC throughout the landscape.

[8] identified that erosion increases the risk of SOC loss. Although some studies have highlighted the impact of erosion on SOC loss, there is a noticeable scarcity of extensive research or case studies that directly correlate soil loss and SOC reserves at the landscape or watershed level in Mexico. Focused case studies could significantly enhance our understanding of the intricate relationship between water erosion and SOC storage dynamics.

The use of geographic information systems (GIS) is essential for predicting soil erosion in landscape and watershed studies. A variety of methodologies and software have been used in these investigations, but the revised universal soil loss equation (RUSLE) model remains the predominant choice for landscape-level erosion modeling [9].

In Mexico, water erosion has affected 52.86% of the nation's land area [10]. This raises a fundamental question: *is there a connection between water erosion and reduced SOC per unit area?* In this vein, the purpose of this study was to investigate the relationship between these factors. This was done by means of the RUSLE predictive model for estimating erosion values. Next, we examined the spatial relationship between erosion and SOC storage in a small watershed located in the state of Oaxaca, Mexico. This information could be used in assisting decision-makers with regard to resource management, in order to preserve the carbon content of soils. Our hypothesis is that water erosion significantly reduces the amount of SOC stored within the watershed per unit area.

Materials and methods

Study area

The study area, called *El Arenal*, is a small 44.6 ha watershed located within the Mixteca Alta region of San Miguel Tulancingo, Oaxaca (Fig. 1), at an altitude of 2200 m. The study area was selected due to its distinctive landscape and apparent erosion indicators, such as gullies and gutters, combined with soil and water conservation practices. According to the INEGI soil map (1:250 000 scale) [11], most of the micro-watershed is classified as a Vertisol. However, field data reveal greater edaphic heterogeneity, with the presence of sandy, ssandy loam, and clay loam textures recorded at various locations. These textures suggest the coexistence of other soil types, such as Litosols and Castañozems.

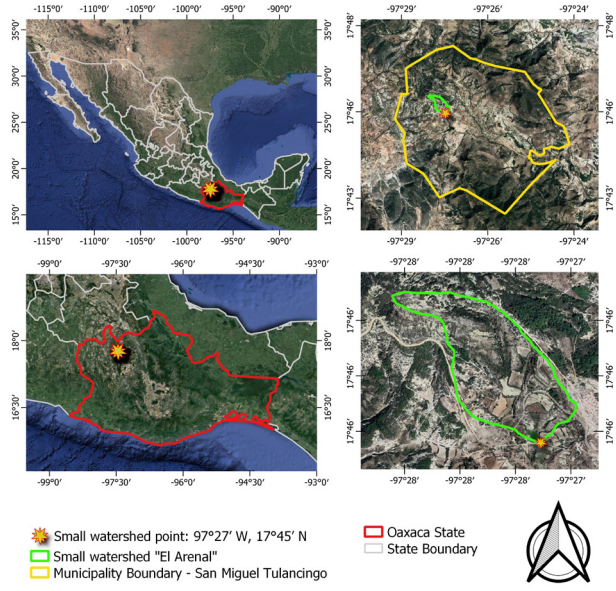

Figure 1. Location of the study area
Source: Authors

Data

Soil organic carbon data

The SOC map used in this study was obtained from a previously validated spatial model developed by [12], using the Smart Map plugin in QGIS, which applies machine learning-based interpolation techniques. In the aforementioned study, a total of 77 geopositioned soil samples were collected from El Arenal at a depth of 0-30 cm. Sampling locations were selected based on accessibility, land use diversity, and topographic variation in order to ensure a representation of the environmental heterogeneity within the watershed. The model reported a mean prediction error (ME) of 0.98 Mg SOC ha^{-1}, a root mean square prediction error (RMSE) of 3.77 Mg SOC ha^{-1}, and a coefficient of determination (R^2) of 0.96, indicating a strong predictive accuracy. This SOC map was incorporated as an input dataset in this study, with the aim of analyzing the spatial relationship between erosion and SOC.

Climate data

Rainfall data for the past 30 years from 11 climate stations within the proximity of the watershed were accessed through the National Meteorological Service's CLICOM database [13].

Soil data

Across the study area, 11 geopositioned soil samples were collected to represent different land use and vegetation conditions. These samples were analyzed to determine particle size distribution – sand, silt, and clay (%) – using the Bouyoucos hydrometer method. In addition, SOC (g kg^{-1}) was measured via the Walkley and Black procedure [14].

Digital elevation model (DEM)

Slope calculations (%) utilized QGIS's slope tool with a 5 m spatial resolution DEM [15].

Satellite imagery

For the analysis, we used Sentinel-2 satellite imagery with a spatial resolution of 10 m, which was acquired on September 26, 2018, from the USGS EarthExplorer platform (https://earthexplorer.usgs.gov/). Atmospheric correction was performed using Luca Congedo's open-source semi-automatic classification plugin (SCP) within QGIS. Subsequently, bands 4 (red) and 8 (near-infrared) were clipped to the extent of the study area.

Methodology

This study was conducted in three phases. In the first phase, a SOC map was generated [12] (Fig. 2). The second phase focused on employing the RUSLE to model erosion estimation, and the third phase established correlations between erosion (X) and SOC (Y).

Spatial modeling of water erosion

Erosion was estimated using the RUSLE. This erosion model is tailored to predict the average annual soil loss due to slope runoff over the long term. The model is illustrated in Eq. (1) [16]–[17]:

$$A = R * K * L * S * C * P \quad (1)$$

where A represents the average soil loss rate (Mg ha^{-1} $year^{-1}$); R denotes the precipitation erosivity factor (MJ.mm.h^{-1}.ha^{-1}.yr^{-1}); K represents the soil erodibility factor (t.h.MJ^{-1}.mm^{-1}); LS combines the factors of slope length and steepness (dimensionless); C denotes the factor for land use and cover (dimensionless); and P is the factor of management practices aimed at preserving the soil (dimensionless).

Rainfall erosivity factor

Rainfall erosivity (R) measures the kinetic energy of raindrops, which cause soil particle displacement [18]. The data show that soil losses from cultivated fields are proportional to storm energy (E) divided by a 30 min maximum intensity (I30) when other factors are constant [17]. The R factor was determined using Eq. (2) [19], as used by [9].

$$R = 0.0483 * P^{1.610} \quad (2)$$

where P is the annual precipitation (mm). To find the R factor, the annual precipitation was interpolated in QGIS using the multilevel B-spline algorithm [20], creating a representative rainfall map. Subsequently, the R factor map was computed using the raster calculator.

Soil erodibility factor

The soil erodibility (K) factor signifies the soil's susceptibility to water-induced erosion.

The K factor was computed using Eq. (3) [16]–[19], as used by [9].

$$K = 27.66 * m^{1.14} * 10\text{-}8 * (12\text{-}a) + 0.0043 * (b\text{-}2) + 0.0033 * (c\text{-}3) \quad (3)$$

where K is the soil erodibility factor (t ha h ha^{-1} MJ^{-1} mm^{-1}); m = (Silt % + Sand %) × (100 - clay %); a refers to the percentage of organic matter; and b is a structure code: 1) very structured, 2) fairly structured, 3) slightly structured, and 4) solid. Additionally, c is the profile permeability code: 1) rapid, 2) moderate to rapid, 3) moderate, 4) moderate to slow, 5) slow, and 6) very slow.

To collect soil data and calculate the K factor, 11 strategically positioned points in the study area were initially selected for soil sampling. The samples were analyzed following Walkley and Black's method [14] for assessing OM, in addition to Bouyoucus method for determining the texture (% sand, silt, and clay).

The K factor was computed and interpolated in QGIS using the IDW method [21]. It exhibited a focal trend, accentuating intense local maxima that coincided with the sampling points.

Slope length and steepness factor (LS)

Steepness and slope length are topographic elements that critically influence soil erosion dynamics. The LS factor is a composite parameter that encompasses the combined effects of slope length (L) and gradient (S) [18]. This factor was computed using a modified adapted from [16], as utilized by [9]. This is shown in Eq. (4).

$$LS = (\text{flow acc} * \text{cellsize}/22.13)^{0.4} * [(\sin(\text{slope} * 3.14/180))/0.0896]^{1.3} \quad (4)$$

Flow accumulation data were first acquired using QGIS's *r.fill* tool from the GRASS module, eliminating depressions in the DEM. Subsequently, the *r.watershed* function was employed to generate the accumulation raster. Calculating the watershed's slope necessitated a slope tool, so a clipped watershed DEM was employed as input in QGIS. Utilizing the raster calculator, LS was then computed using the *flow acc* and *slope* layers. This comprehensive approach to LS factor computation provided a more nuanced understanding of the topographical influences on erosion within the study area.

Crop management factor

The crop management (C) factor is a measure of the percent soil loss potential based on the protection afforded by different land-cover types. Higher C factor values indicate a lack of vegetation cover, thereby increasing the risk of significant soil loss. Vegetation cover is a key factor in erosion control since it intercepts precipitation, enhances infiltration, and mitigates the erosive impact of rainfall [18]. To quantify the C factor, we employed Eq. (5), introduced by [22] and employed by [9].

$$C=0.431-0.805 * NDVI \quad (5)$$

The normalized difference vegetation index (NDVI) was fundamental in this calculation. This index was defined by [23] and employed in this work by means of Eq. (6).

$$NDVI = (NIR - RED) / (NIR + RED) \quad (6)$$

Here, NIR stands for the reflectance in the near-infrared band (%), while RED is the reflectance in the red band (%). B8 Sentinel-2 imagery corresponds to the NIR band, and B4 corresponds to the R band, both with a spatial resolution of 10 m. The NDVI was computed via QGIS's *i.vi* module, and the C factor, obtained using the Eq. (5), was obtained using the raster calculator. This approach offered a comprehensive understanding of how different land-cover types contribute to erosion risk within the study area.

Conservation practices factor

The conservation practices (P) factor assesses the efficacy of soil protection against erosion through management practices, as these practices reduce runoff and consequently limit soil loss [18]. In this work, the calculation of this factor involved the manual digitization of a Google Earth image within QGIS. A subsequent field visit was conducted to validate areas with soil and water conservation initiatives. Moreover, digitization was refined using land knowledge obtained during field campaigns. In QGIS, reclassification was conducted using the percentage values of the slope map, as well as zone-based statistics, to compute the mean slope value for each digitized polygon. In the attribute table of the generated polygons provided the corresponding P values. These values were determined based on Table I, *i.e.*, according to the average slope grades and their corresponding P factor values, as proposed by [24] and adopted by [25]. This methodological approach captured the nuanced interplay between management practices, slope gradients, and erosion mitigation within the study area.

Table I. P factor values for contouring, strip-cropping, and terracing focusing on slope classes

Slope (%)	Conservation Practices (P Factor)		
	Contouring	Strip Cropping	Terracing
0.0-7.0	0.55	0.27	0.10
7.0-11.3	0.60	0.30	0.12
11.3-17.6	0.80	0.40	0.16
17.6-26.8	0.90	0.45	0.18
>26.8	1	0.50	0.20

Source: [24]

Correlation between erosion and SOC storage

Soil samples were gathered during field visits in order to quantify SOC levels. From this sampling, 50 georeferenced points were randomly selected (Fig. 2) and positioned on the erosion map.

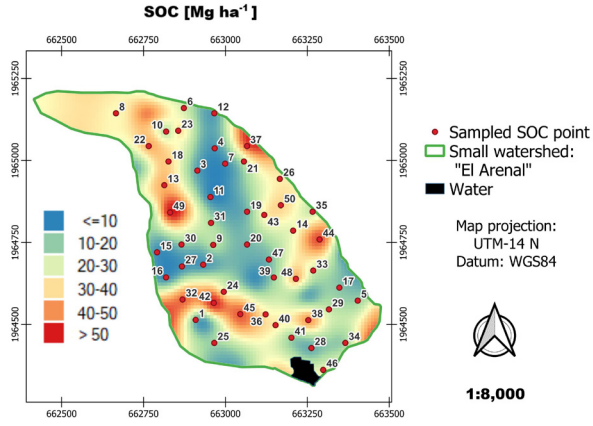

Figure 2. SOC map in Mg ha^{-1}. The 50 georeferenced points correlating erosion and SOC are shown in red.
Source: [12]

Using QGIS's point sampling tool, the estimated erosion values were derived for each point and associated with their corresponding erosion classification values (null, light, moderate, and high). The correlation analysis considered X (erosion, Mg ha^{-1} year^{-1}) and Y (SOC, Mg ha^{-1}). To initiate the examination, a descriptive statistical analysis was performed, accompanied by the elaboration of a scatter plot (X,Y), a histogram paired with a normal curve, and a Q-Q plot to assess data normality. Normality was evaluated using the Shapiro-Wilk test [26]–[27]. Since our data did not follow a normal distribution, the Kendall *tau* correlation coefficient

test (KTCCT) was applied. The Kendall correlation coefficient and its corresponding p-values guided the decision between the two hypotheses, *i.e.*, H_0 (no association) and H_1 (correlation). The Kendall coefficient ranges from -1 to 1, where positive values indicate a positive association and negative ones denote a negative association. The statistical computations presented in this section were conducted using the R Studio software [28]. This rigorous approach ensured a comprehensive analysis of the relationship between SOC and erosion levels, thereby yielding insights into their dynamic interdependence.

Results

The R factor is shown in Fig. 3a. The minimum, maximum, and average values for R and precipitation were (1302, 565), (1356, 579), and (1325, 571) in MJ.mm.h^{-1}.ha^{-1}.yr^{-1} and mm, respectively. The upper regions of the small watershed exhibited the highest R values, which correlated with the zones of maximum precipitation.

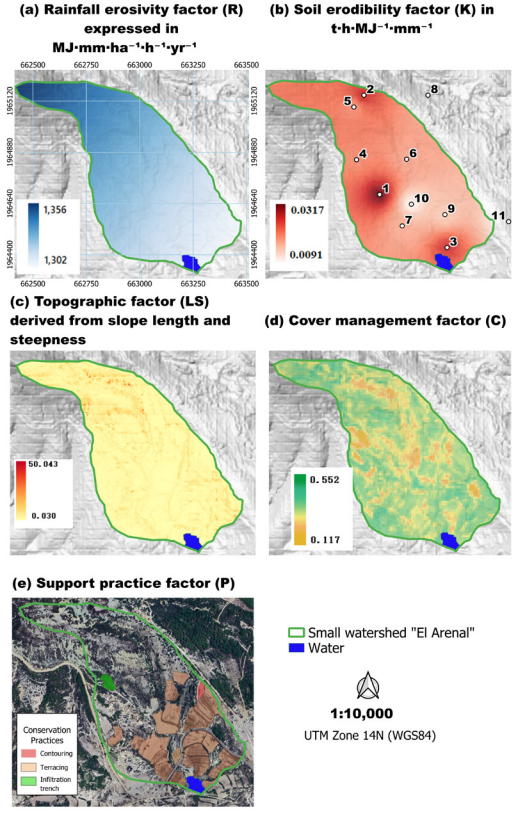

Figure 3. Spatial representation of the five input factors used in the RUSLE model to estimate soil erosion in the El Arenal micro-watershed
Source: Authors

In Fig. 3b, the *K* factor shows variation within the small watershed, with values ranging from 0.0091 to 0.0317 t.ha.h.MJ^{-1}.mm^{-1} and an average of 0.0197 t.ha.h.MJ^{-1}.mm^{-1}.

Table II provides an overview of the sampled soil points, their corresponding land use and vegetation, the soil texture values, and the estimated K factor. Notably, the latter was the lowest in the bare soil areas and the highest in the agricultural zones.

Table II. K values estimated by soil texture class

ID	Land use and vegetation	Texture	K-RUSLE
1	Rainfed agriculture	Loam	0.0317
2	Thorn scrub	Clay loam	0.0264
3	Rainfed agriculture	Sandy clay loam	0.0263
4	Adult pine plantation	Sandy clay loam	0.0199
5	Gallery vegetation	Sandy clay loam	0.0196
6	Gallery vegetation	Sandy loam	0.0179
7	Rainfed agriculture	Clay loam	0.0177
8	Adult pine plantation	Sandy clay loam	0.0159
9	Rainfed agriculture	Sandy loam	0.0150
10	Bare soil	Sandy loam	0.0111
11	Bare soil	Sandy loam	0.0091

Source: Authors

The LS factor (Fig. 3c) shows values ranging from 0.030 to 23 045, with an average of 2.31. Notably, the elevated values were concentrated in regions denoted as *flow accumulation zones*, mainly along river courses (Fig. 4).

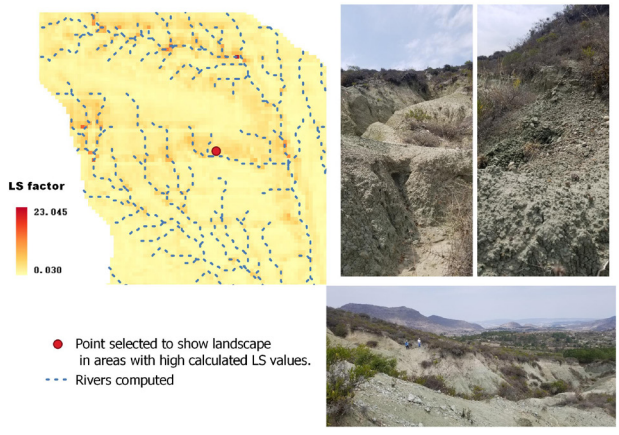

Figure 4. Point selected to show a landscape with high values of LS factor
Source: Authors

The C factor (Fig. 3d) exhibits a range of values spanning from 0.117 to 0.552, with an average of 0.322. These C values, corresponding to diverse soil and vegetation uses in the small watershed, indicate the following categories: bare soil (0.488), gallery vegetation (0.314), thorn scrub (0.328), rainfed agriculture (0.295), and adult pine plantation (0.129).

The P factor in Fig. 3e corresponds to slope-related values. A total of 18 polygons were digitized under field supervision to obtain these values. Table III illustrates the direct relationship between an increasing slope and a higher P factor.

Table III. P values associated with slope (%)

Polygon	PCWS	Slope (%)	P factor
1	None	16.1	1
2	Land terrace	26.48	0.2
3	Land terrace	28.97	0.2
4	Land terrace	17.02	0.18
5	Land terrace	17.44	0.18
6	Land terrace	17.82	0.18
7	Land terrace	11.13	0.16
8	Contouring	12.08	0.16
9	Land terrace	14.63	0.16
10	Land terrace	8.81	0.12
11	Land terrace	9.13	0.12
12	Land terrace	9.55	0.12
13	Land terrace	5.24	0.1
14	Land terrace	5.87	0.1
15	Land terrace	6.02	0.1
16	Land terrace	6.74	0.1
17	Infiltration trench	7.05	0.1

Source: Authors

Spatial modelling of erosion estimation

Fig. 5 shows the spatial distribution of soil erosion in the study area. The minimum, maximum, and average values were 0.19, 266.99, and 17.44 Mg ha^{-1} year^{-1}, respectively. The cumulative erosion for the entirety of the watershed was estimated at 305 693 t. The average erosion-related SOC values (Mg ha^{-1}) by classification are as follows: null (31.79), light (22.36), moderate (16.19), and high (5.22).

The average erosion values (in Mg ha^{-1} year^{-1}) associated with different soil and vegetation types are as follows: bare soil (55.02), thorn scrub (29.50), gallery vegetation (17.84), adult pine plantation (5.76), and rainfed agriculture (2.31). The lowest erosion value is linked to flat slopes within agricultural areas that have implemented soil and water conservation practices such as land terracing. On the other hand, erosion values exceeding 200 Mg ha^{-1} year^{-1} are concentrated in the northern zone of the small watershed, characterized by high R and LS values, as well as by the absence of conservation practices.

Correlation between erosion and SOC storage

The dataset, comprising 50 points, can be observed in Fig. 6 and Table V, which detail the estimated erosion and measured SOC values. A visual comparison of erosion and SOC is depicted in Fig. 6 by means of a bar graph. This graph shows that in 35 out of 50 instances (70% of the sample), as erosion decreases, the SOC tends to increase.

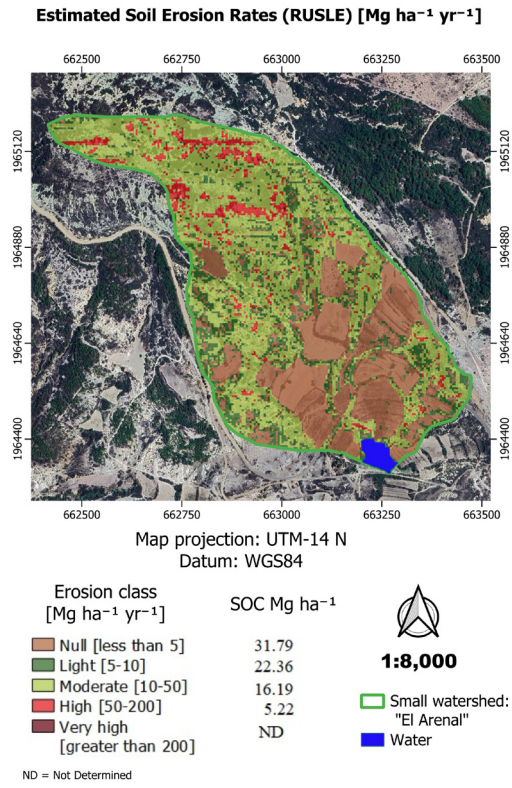

Figure 5. Spatial distribution of the estimated soil erosion rates (Mg ha^{-1} yr^{-1}) and soil organic carbon (SOC) content (Mg ha^{-1}) across the El Arenal micro-watershed
Source: Authors

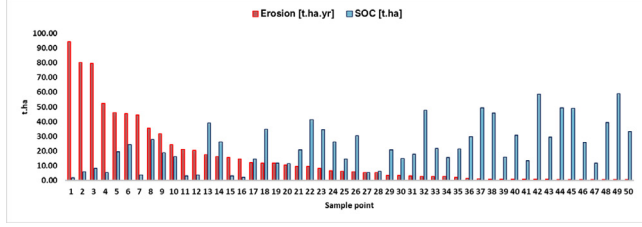

Figure 6. Graphical comparison of erosion and SOC
Source: Authors

A scatter plot was created to illustrate the connection between erosion and SOC. This plot reveals a relatively weak correlation, with an R^2 value of 0.21. Descriptive statistics for both variables are presented Table IV. Notably, the mean for both variables exceeds the median, indicating an asymmetric distribution.

Table IV. Descriptive statistics and Shapiro-Wilk test for erosion and SOC

Statistics	Erosion (X)	SOC (Y)
Number	50.00	50,00
Addition	770.63	1 158.21
Half	15.41	23.16
Median	6.10	20.60
Stdvd (pop)	22.12	15.53
Stdvd (sample)	22.34	15.69
Minimum	0.19	1.58

Maximum	94.40	59.07
Range	94.21	57.49
Minority	0.19	1.58
Most	0.19	1.58
Variety	50.00	50.00
Q1	0.87	11.57
Q3	17.62	33.32
IQR	16.75	21.75
Missing (null) values	0.00	0.00
P-value (Shapiro W)	6.907e-9	0.006948
W (Shapiro W)	0.6956	0.9326

Source: Authors

Fig. 7 shows the statistical relationship between soil erosion and SOC. A moderate negative correlation was observed (r=-0.46), with the SOC decreasing as erosion increased (Fig. 7a). The erosion data exhibited a right-skewed distribution (Fig. 7b), which was confirmed by the deviation from normality in the Q-Q plot (Fig. 7c). In contrast, the SOC values followed a more symmetrical and near-normal distribution, as shown in Figs. 7d and 7e.

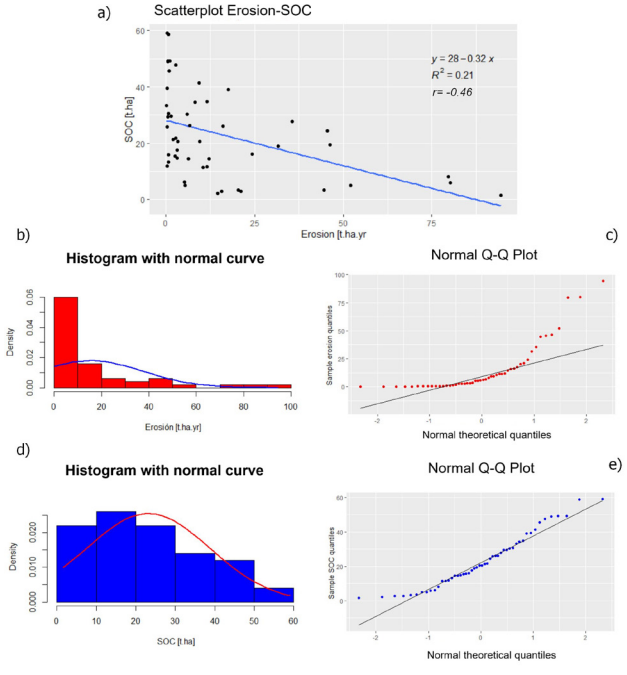

Figure 7. An asymmetric distribution was observed in both the histograms and Q-Q plots. a) Scatterplot illustrating the negative linear correlation between soil erosion (Mg ha^{-1} yr^{-1}) and SOC (Mg ha^{-1}), including the regression line, the equation, the coefficient of determination (R^2=0.21), and Pearson's correlation coefficient (r=-0.46). b) Histogram with the density curve of the erosion values, indicating a right-skewed distribution. c) Normal Q-Q plot showing that the erosion values deviate from normality, particularly in the upper quantiles. d) Histogram with a density curve of SOC values, approximating a normal distribution. e) Normal Q-Q plot confirming that the SOC values closely follow a normal distribution.
Source: Authors

Regarding the normality test (Shapiro-Wilk), the results for the variables X and Y were as follows: W (50) = 0.70, p < 0.001; W (50) = 0.93, p = 0.007. This indicates that the data do not follow a normal distribution in either case. Therefore, the data can be analyzed using non-parametric tests.

As for the non-parametric data, Kendall's rank correlation coefficient was utilized. The results for Kendall's *tau* are as follows: z = -3.9566, p-value = 7.603e-05, and *tau* = -0.386. This value of *tau* supports the alternative hypothesis, as it is not equal to zero. The results demonstrate a negative correlation, implying that the variables move in opposite directions

Table V presents the details of the 50 sampled points, *i.e.*, data on erosion, SOC storage, land use, vegetation, and soil and water conservation practices. This table reveals that areas with higher erosion rates tend to exhibit a lower SOC storage. Specifically, points 38 to 50 show a higher frequency of terraces, which aligns with agricultural areas and corresponds to reduced soil loss.

Table V. Sampled points and their corresponding data

ID	E	SOC	LSV	SWCP	ID	E	SOC	LSV	SWCP
1	94.40	1.58	Bs	N	26	5.88	30.38	App	N
2	80.20	6.02	Ts	N	27	5.33	5.11	Ts	N
3	79.53	8.17	Ts	N	28	5.27	6.24	Ra	T
4	52.11	5.10	Gv	N	29	3.43	20.56	Ra	T
5	46.25	19.35	Ts	N	30	3.15	14.80	Ts	N
6	45.56	24.37	Ts	N	31	3.12	17.68	Gv	N
7	44,62	3.52	Ts	N	32	2.79	47.66	Ra	T
8	35.63	27.78	Ts	N	33	2.69	21.79	Ra	T
9	31.66	18.88	Gv	N	34	2.62	15.45	Ra	T
10	24.28	16.16	Gv	N	35	2.03	21.36	Ra	C
11	21.05	2.91	Ts	N	36	1.39	29.63	Gv	N
12	20.30	3.49	Ts	N	37	1.08	49.20	App	N
13	17.62	39.13	Ts	N	38	0.87	45.68	Ra	T
14	16.10	26.09	Ts	N	39	0.77	15.83	Ra	T
15	15.65	2.88	Bs	N	40	0.66	30.62	Ra	T
16	14.54	2.17	Ra	N	41	0.65	13.35	Ra	T
17	12.11	14.52	App	N	42	0.63	58.69	Ra	T
18	11.65	34.82	Ts	N	43	0.59	29.48	Ra	T
19	11.53	11.57	Gv	N	44	0.55	49.23	Ra	T
20	10.51	11.38	Gv	N	45	0.50	49.03	Ra	T
21	9.51	20.65	App	N	46	0.35	25.77	Ra	T
22	9.30	41.33	Ts	N	47	0.30	11.82	Ra	T

23	8.16	34.44	Gv	N	48	0.29	39.45	Ra	T
24	6.65	26.20	Ra	N	49	0.25	59.07	App	IT
25	6.33	14.56	Ts	N	50	0.19	33.32	Ra	T

ID: identification of the sampled point, E: erosion (Mg ha^{-1} year^{-1}), SOC: soil organic carbon (Mg ha^{-1}), LSV: land use and vegetation, SWCP: soil and water conservation practices, Bs: bare soil, Ts: thorn scrub, Gv: gallery vegetation, Ra: rainfed agriculture, App: adult pine plantation, N: none, T: terracing, C: contouring, IT: infiltration trench.
Source: Authors

Figure 8. View of some representative sites.
Source: Authors

Discussion

The results of this study provided significant insights into the erosion-SOC relationship. Kendall's *tau* value (-0.39), for instance, revealed a negative correlation. This implies that, as erosion increases, SOC tends to decrease. This negative correlation can be attributed to the erosion process, including initiation, transport, and deposition, which can impact the loss and gain of SOC within the watershed. [1] highlighted the significant impact of water erosion on the transport of organic carbon. This impact begins with the decomposition of aggregates, leading to the exposure of SOC. During this process, colloidal fractions such as fine silt, clay, and SOC are eliminated. The sediment, along with carbon, undergoes redistribution and is eventually deposited in depression areas. In our study area, this phenomenon was primarily observed in areas with greater soil loss, which tend to coincide with concave zones such as slopes. Regarding these sites, [29] indicated that a high cumulative intensity of water erosion reduces the vegetation cover through the formation of streams or ravines, decreasing the thickness of the soil and eliminating the upper layer of fertile soil, which in turn leads to a decrease in SOC. The RUSLE model identified these areas as having higher LS and C values, predominantly consisting of bare soil and thorn scrub (Fig. 3).

Studies suggest an initial loss of SOC during erosion. Nevertheless, this lost carbon is transported to flatter areas [1], [29], [30]. In our study area, this trend is aligned with the lower part of the watershed where agricultural areas are located. According to [31] and [32], these locations also correspond to the presence of soil and water conservation practices, which create conditions for carbon storage.

Previous research conducted in the same watershed [12] demonstrated that SOC storage is strongly influenced by land cover and soil type. For example, gallery vegetation and pine plantations exhibited higher SOC values (up to 31.8 Mg ha^{-1}), while intensively cultivated areas stored much lower values (around 5.2 Mg ha^{-1}). These patterns coincided with soil classification: Vertisols with fine textures supported a greater SOC retention, whereas Litosols and sandy soils were associated with a reduced SOC content. These findings are consistent with broader studies. [6] reported that nearly 50% of Mexico's SOC is concentrated in the upper 30 cm of the soil, which makes it highly vulnerable to erosion. Similarly, [7] emphasized that soil erosion processes can significantly deplete SOC stocks through the detachment and oxidation of OM. [31] also observed higher SOC values in vegetated zones when compared to croplands, and [32] identified land use as a key factor influencing SOC accumulation, even in terraced systems. Our findings align with these observations: areas with high erosion – mainly bare soils and scrublands – are linked to low SOC values, while depositional zones with conservation practices such as terracing promote SOC accumulation. These outcomes underscore the importance of considering both edaphic and vegetation factors in land management strategies aimed at improving carbon retention and reducing erosion at the watershed scale.

This is line with [2]: erosion-induced carbon storage is supported by two key mechanisms. First, dynamic replacement involves the replacement of eroded carbon with new carbon, such as OM from vegetation. This is especially relevant in cultivated areas. Second, reduced decay rates in depositional environments contribute to long-term carbon storage.

This increased carbon storage takes place through a combination of dynamic replacement and reduced decomposition, which ultimately contributes to an overall carbon storage increase, despite the initial carbon loss due to erosion, as seen in sites 1 and 3 (Fig. 7 and Table V). These dynamics reinforce the notion that erosion culminates in deposition, particularly in agricultural zones. Conservation practices like terracing amplify carbon storage benefits, as exemplified in sites 38 and 42. These findings align with [30], who explains how erosion and deposition redistribute sediment and SOC in agricultural landscapes.

However, it must be acknowledged that, while the correlation exists, it is relatively weak. Some cases, such as sites 39 and 47, showed a lower carbon content in agricultural areas with terraces. Here, the absence of dynamic replacement due to limited recent cultivation (uncultivated agricultural land) prevented SOC storage. Despite soil and water conservation efforts, these sediment-filled areas retain less SOC, which underscores the importance of active soil management in promoting dynamic carbon replacement. According to the study conducted by [32], SOC storage resulting from terracing is primarily influenced by land use.

This discussion highlights the intricate interactions between erosion, sedimentation, and carbon storage within landscapes, emphasizing that natural processes can yield unexpected carbon dynamics. It is crucial to consider the importance of accounting for both erosion and deposition when evaluating carbon budgets. However, one limitation of this research lies in the need to validate the spatial erosion model in the field.

Future research could investigate whether the SOC within sediment layers buried deep in soil and water conservation areas qualifies as a CO_2 sink. This proposition arises from the stabilization of carbon within oxygen-limited environments, facilitated by organisms responsible for decomposition, in line with [33].

Conclusion

This study examined the spatial relationship between water erosion and SOC storage in a small watershed using the RUSLE model and geostatistical analysis. According to the initial hypothesis, erosion intensity is negatively related to SOC levels. In approximately 70% of our data, lower erosion rates corresponded to higher SOC values, with a Kendall *tau* correlation coefficient of -0.39. This inverse trend was attributed to erosion-induced aggregate breakdown and SOC detachment, followed by its redistribution across the landscape.

Despite the observed relationship, the correlation was moderate, suggesting that other variables such as vegetation cover, land use, and soil texture also influence SOC dynamics. Our findings demonstrate that erosion does not always lead to an irreversible loss of SOC. Instead, it can contribute to the storage of carbon in depositional zones under favorable conditions. In low-oxygen environments, mechanisms such as dynamic carbon replacement from vegetation and reduced decomposition rates enhance SOC retention, particularly in areas managed with conservation practices such as terracing.

The findings of this study demonstrate the importance of integrating erosion control and carbon management into land use planning. In the future, it would be beneficial to explore whether the SOC stored in buried sediment layers under conservation structures can act as a long-term CO_2 sink, which could contribute to the mitigation of climate change.

CRediT author statement

- OTAS conceived and elaborated the manuscript, conducted field data collection, performed spatial and statistical data processing, and wrote the original draft.
- JPN provided overall conceptual direction, supervised the methodological framework, and critically revised the manuscript.
- CAAS actively contributed to the content review and substantially improved the structure and clarity of the article.
- AIMR supported the review process, particularly regarding results interpretation and scientific framing.

Conflicts of interest

There is no conflict of interest to declare.

Data availability

The data used in this study can be provided upon request to the corresponding author.

References

[1] R. Lal, "Fate of soil carbon transported by erosional processes," *Appl. Sci.*, vol. 12, no. 1, p. 48, Dec. 2021. http://doi.org/10.3390/app12010048

[2] S. Doetterl, A. A. Berhe, E. Nadeu, Z. Wang, M. Sommer, and P. Fiener, "Erosion, deposition and soil carbon: A review of process-level controls, experimental tools and models to address C cycling in dynamic landscapes," *Earth-Sci. Rev.*, vol. 154, pp. 102–122, Mar. 2016. http://doi.org/10.1016/j.earscirev.2015.12.005

[3] R. Lal, "Accelerated soil erosion as a source of atmospheric CO2," *Soil Tillage Res.*, vol. 188, pp. 35–40, May 2019. http://doi.org/10.1016/j.still.2018.02.001

[4] C. Lefèvre, F. Rekik, V. Alcantara, and L. Wiese, *Soil organic carbon: The hidden potential*. Rome, Italy: Food and Agriculture Organization of the United Nations, 2017.

[5] H. Burbano Orjuela, "El carbono orgánico del suelo y su papel frente al cambio climático," *Rev. Cienc. Agríc.*, vol. 35, no. 1, p. 82, Jun. 2018. http://doi.org/10.22267/rcia.183501.85

[6] F. Paz and J. Etchevers, "Distribución a profundidad del carbono orgánico en los suelos de México," *Terra Latinoam.*, vol. 34, no. 3, pp. 339–335, 2016. http://www.scielo.org.mx/scielo.php?script=sci_arttext&pid=S0187-57792016000300339&lng=es&tlng=es

[7] K. R. Olson, M. Al-Kaisi, R. Lal, and L. Cihacek, "Impact of soil erosion on soil organic carbon stocks," *J. Soil Water Conserv.*, vol. 71, no. 3, pp. 61A–67A, May 2016. http://doi.org/10.2489/jswc.71.3.61A

[8] L. Cui, X. Li, J. Lin, G. Guo, X. Zhang, and G. Zeng, "The mineralization and sequestration of soil organic carbon in relation to gully erosion," *CATENA*, vol. 214, art. 106218, Jul. 2022. http://doi.org/10.1016/j.catena.2022.106218

[9] D. B. Tiruwa, B. R. Khanal, S. Lamichhane, and B. S. Acharya, "Soil erosion estimation using geographic information system (GIS) and revised universal soil loss equation (RUSLE) in the Siwalik Hills of Nawalparasi, Nepal," *J. Water Clim. Change*, vol. 12, no. 5, pp. 1958–1974, Aug. 2021. http://doi.org/10.2166/wcc.2021.198

[10] INEGI (National Institute of Statistics and Geography), "Soil erosion dataset, scale 1:250 000 series I, national continuum," 2014. [Online]. Available: https://www.inegi.org.mx/app/biblioteca/ficha.html?upc=702825004223

[11] INEGI (National Institute of Statistics and Geography), "Soil map, scale 1:250,000. National continuum," 2002-2006. [Online]. Available: https://www.inegi.org.mx/app/biblioteca/ficha.html?upc=794551131916

[12] O. Aguirre-Salado, J. Pérez-Nieto, C. Aguirre-Salado, and A. Monterroso-Rivas, "Factors regarding the spatial variability of soil organic carbon in a Mexican small watershed," *Rev. Fac. Agron. Univ. Zulia*, vol. 41, no. 1, art. e244101, Dec. 2023. http://doi.org/10.47280/RevFacAgron(LUZ).v41.n1.01

[13] CLICOM, "Daily climate data from the CLICOM of the SMN through its CICESE web platform," 2023. [Online]. Available: https://cucapa-clicom.cicese.mx/mapa.html

[14] A. Walkley and C. A. Black, "An examination of the Degtjareff method for determining soil organic matter and a proposed modification of chromic acid titration method," *Soil Sci.*, vol. 37, pp. 29–38, 1934.

[15] INEGI (National Institute of Statistics and Geography), "Digital surface-type elevation model with 5m resolution derived from satellite and airborne remote sensing data," 2017. [Online]. Available: https://www.inegi.org.mx/app/biblioteca/ficha.html?upc=889463542605

[16] W. H. Wischmeier and D. D. Smith, *Predicting rainfall erosion losses – A guide to conservation planning*. Washington, DC, USA: Department of Agriculture, Science and Education Administration, 1978.

[17] K. G. Renard, G. R. Foster, G. A. Weesies, D. K. McCool, and D. C. Yoder, *Predicting soil erosion by water: A guide to conservation planning with the revised universal soil loss equation* (*RUSLE*). Washington, DC, USA: US Government Printing Office, 1997.

[18] C. A. Aguirre-Salado *et al.*, "Improving identification of areas for ecological restoration for conservation by integrating USLE and MCDA in a GIS-environment: A pilot study in a priority region northern Mexico," *ISPRS Int. J. Geo-Inf.*, vol. 6, no. 9, art. 262, Aug. 2017. http://doi.org/10.3390/ijgi6090262

[19] K. G. Renard and J. R. Freimund, "Using monthly precipitation data to estimate the R-factor in the revised USLE," *J. Hydrol.*, vol. 157, no. 1, pp. 287–306, 1994.

[20] S. Lee, G. Wolberg, and S. Y. Shin, "Scattered data interpolation with multilevel B-splines," *IEEE Trans. Vis. Comput. Graph.*, vol. 3, no. 3, pp. 228–244, Sep. 1997. http://doi.org/10.1109/2945.620490

[21] N. Efthimiou, "The new assessment of soil erodibility in Greece," *Soil Tillage Res.*, vol. 204, art. 104720, Oct. 2020. http://doi.org/10.1016/j.still.2020.104720

[22] S. M. De Jong, L. C. Brouwer, and H. T. Riezebos, "Erosion hazard assessment in the La Peyne Catchment, France," Department of Physical Geography, University of Utrecht, Utrecht, The Netherlands, 1998. [Online]. Available: https://research.wur.nl/en/publications/erosion-hazard-assessment-in-the-la-peyne-catchment-france

[23] C. J. Tucker, "Red and photographic infrared linear combinations for monitoring vegetation," *Remote Sens. Environ.*, vol. 8, pp. 127–150, 1979.

[24] G. Shin., "The Analysis of Soil Erosion Analysis in Watershed Using GIS," PhD dissertation, Gang-Won National University, Chuncheon, Korea, 1999. [Online]. Available: https://www.scirp.org/reference/referencespapers?referenceid=3870069

[25] F. Karamage, C. Zhang, T. Liu, A. Maganda, and A. Isabwe, "Soil Erosion Risk Assessment in Uganda," *Forests*, vol. 8, no. 2, p. 52, Feb. 2017. http://doi.org/10.3390/f8020052

[26] S. S. Shapiro and M. B. Wilk, "An analysis of variance test for normality (complete samples)," *Biometrika,* vol. 52, no. 3/4, pp. 591–611, 1965.

[27] H. Hernandez, "Testing for Normality: What is the Best Method?," 2021. [Online]. Available: https://doi.org/10.13140/RG.2.2.13926.14406

[28] RStudio Team, "RStudio: Integrated development for R," 2023. [Online]. Available: http://www.rstudio.com/

[29] L. Liu, Q. Zhang, Q. Liu, and Z. Li, "Is soil an organic carbon sink or source upon erosion, transport and deposition?," *Eur. J. Soil Sci.*, vol. 74, no. 1, art. e13344, Jan. 2023. http://doi.org/10.1111/ejss.13344

[30] F. M. S. A. Kirkels, L. H. Cammeraat, and N. J. Kuhn, "The fate of soil organic carbon upon erosion, transport and deposition in agricultural landscapes — A review of different concepts," *Geomorphology*, vol. 226, pp. 94–105, Dec. 2014. http://doi.org/10.1016/j.geomorph.2014.07.023

[31] E. Bojago, M. W. Delango, and D. Milkias, "Effects of soil and water conservation practices and landscape position on soil physicochemical properties in Anuwa watershed, Southern Ethiopia," *J. Agric. Food Res.*, vol. 14, art. 100705, Dec. 2023. http://doi.org/10.1016/j.jafr.2023.100705

[32] D. Chen, W. Wei, S. Daryanto, and P. Tarolli, "Does terracing enhance soil organic carbon sequestration? A national-scale data analysis in China," *Sci. Total Environ.*, vol. 721, art. 137751, Jun. 2020. http://doi.org/10.1016/j.scitotenv.2020.137751

[33] M. Mekonnen and M. Getahun, "Soil conservation practices contribution in trapping sediment and soil organic carbon, Minizr watershed, northwest highlands of Ethiopia," *J. Soils Sed.*, vol. 20, no. 5, pp. 2484–2494, May 2020. http://doi.org/10.1007/s11368-020-02611-5